Mansell, Rhodri; Huhtasalo, Joonatan; Ameziane, Maria; van Dijken, Sebastiaan

Skyrmion size and density in lattices

Skyrmion size and density in lattices

View Online Export Citation CrossMark

Rhodri Mansell,[a] Joonatan Huhtasalo, Maria Ameziane, and Sebastiaan van Dijken

AFFILIATIONS

NanoSpin, Department of Applied Physics, Aalto University School of Science, P.O. Box 15100, FI 00076 Aalto, Finland

[a]Author to whom correspondence should be addressed: rhodri.mansell@aalto.fi

ABSTRACT

The effect of changing magnetic parameters on the size and density of skyrmions in a hexagonal lattice is investigated using micromagnetic simulations. Achieving control of the skyrmion density, for instance, by applied voltages, is a route to magnetic neuromorphic computing devices. Here, we show how small changes in the uniaxial magnetic anisotropy and Dzyaloshinskii–Moriya interaction lead to large changes in the skyrmion size and density, which occurs for parameters that do not support isolated skyrmions. The effect of a grain structure on the density of skyrmions is modeled through the introduction of a locally varying anisotropy. This shows that a higher density of skyrmions is favored for a wider distribution of magnetic anisotropy. The results provide a clear understanding of systems where the skyrmion density can be externally controlled and assist the design of functional skyrmion-based devices.

I. INTRODUCTION

Magnetic skyrmions have been extensively studied for memory and logic device applications.[1–3] They are also interesting as a topological magnetic particle displaying rich physical properties, such as the skyrmion Hall effect.[4] In thin films, skyrmions are stabilized by the competition between magnetic energy terms: the exchange interaction, uniaxial anisotropy, dipolar fields, and the Dzyaloshinskii–Moriya interaction (DMI).[1] One area of interest is creating skyrmion devices, which can be controlled by an applied voltage.[5–7] Skyrmions can be nucleated and moved by electrical currents,[2,3] but manipulating skyrmions with applied voltages would remove the effects of Joule heating and allow devices to operate with greater energy efficiency.[6,8]

Despite a large number of device proposals, the experimental implementation of digital logic with skyrmions has been limited, often due to the effects of disorder, which can lead to strong skyrmion pinning.[9] Recently, skyrmion devices which exploit a different computing paradigm, that of reservoir computing,[10] have been demonstrated.[11–13] Here, the response of the magnetic state acts as a reservoir with a high inherent dimensionality, which can be controlled by inputs such as magnetic fields,[12] applied currents,[11] or voltages.[13] Necessary features of the reservoir for neuromorphic computing are a non-linear response to the input and a memory effect.[10] In terms of skyrmion density-based devices, these features translate into a non-linear dependence of the skyrmion density on the input strength and duration and hysteretic behavior in the

skyrmion density when the input is swept. By training an output layer, it has been shown that these devices can be used to implement classification tasks[11–13] as well as predicting the dynamics of a chaotic system.[13]

Previously, it has been shown in a variety of different material systems that the density of skyrmions can be controlled by applied voltages.[5,7,14–17] This effect can generally be attributed to changes in the uniaxial anisotropy constant[5] or the DMI.[15] The skyrmion density is also controllable via applied magnetic fields[18–20] or by changing the temperature, which acts to alter the exchange stiffness, magnetic anisotropy, or DMI.[18,21]

As well as experimental results, significant work has been carried out using simulations and theoretical calculations. For isolated skyrmions, the change of the skyrmion size as a function of the magnetic parameters has been derived,[22] which shows that decreasing anisotropy or increasing DMI leads to larger skyrmions. In contrast to the results for isolated single skyrmions, simulations on dense skyrmion lattices, based on different physical systems, indicate that decreasing magnetic anisotropy and increasing DMI lead to smaller skyrmions.[20,23,24] In this paper, we investigate the skyrmion energy as a function of skyrmion size for fixed skyrmion density in order to extract the relationship between the size and density of skyrmions for different sets of material parameters.

Our approach fixes the skyrmion density in each simulation. This is different from the more typical approach whereby the density is allowed to evolve from a defined starting position either

through annihilation or nucleation of skyrmions.[19,23,25] The common approach does not necessarily lead to an equilibrium density of skyrmions due to the finite energy required to nucleate or annihilate skyrmions. Moreover, it can lead to different skyrmion sizes and densities due to the effects of the size of the simulation and the use of periodic boundary conditions.

II. METHODS

The magnetic parameters used in this paper are based on those determined from experimental magneto-ionic devices showing voltage control of the skyrmion density.[17] The experimentally studied sample consisted of a Ta (2 nm)/Pt (4 nm)/CoFeB (0.9 nm)/Pt (0.2 nm)/LiPON (100 nm)/SiN (1 nm)/Pt (4 nm) structure, where the observed changes from voltages applied across the LiPON layer are assumed to come from changes to the uniaxial anisotropy or the DMI due to the accumulation of Li ions at the CoFeB/Pt/LiPON interfaces. In this paper, micromagnetic simulations are used to investigate how changing the uniaxial anisotropy alters the size and density of skyrmions in the lowest energy state. The simulations are carried out using the MuMax3 package.[26,27] A cell size of 2.5 nm in the x- and y-directions and 0.9 nm in the z-direction is used. A single cell in the z-direction is used to match the experimental layer thickness, as described above. The saturation magnetization, M_s, is 1.209 MA/m, as derived from experiments, with the damping parameter, α, set to 0.1. The uniaxial anisotropy, K_u, DMI and exchange constant, A_{ex}, are varied around the experimentally determined values (relating to a non-skyrmion state) of 9.94×10^5 J/m^3 and 0.74 mJ/m^2 and is 14 pJ/m, respectively.

To study the effect of skyrmion density, a hexagonal skyrmion lattice was created. This was achieved by using a rectangular simulation grid with a ratio of $\sqrt{3}$ between the two sides (within discretization limits). By placing skyrmions at the center of each face, a hexagonal lattice is formed when periodic boundary conditions are applied. An example is shown in Fig. 1(a), where a single cell is outlined in blue. The tessellated pattern created by the periodic boundary conditions is shown as well. In order to find the minimum energy state, skyrmions of different sizes are nucleated and the system is relaxed. In other words, the local minimum
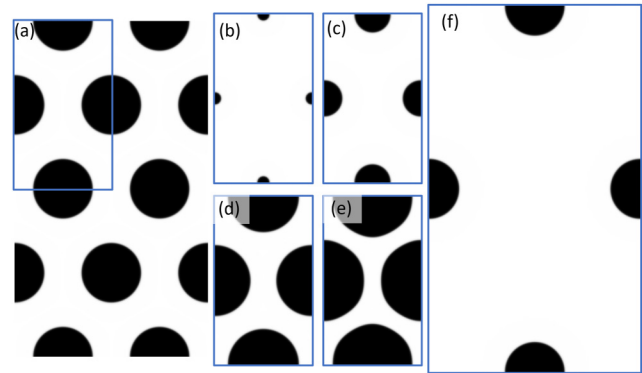

FIG. 1. (a) Geometry used to test the effects of skyrmion density. The skyrmions are the black circles (magnetization pointing down) with a skyrmion diameter of around 846 nm positioned in a 1375 × 2382.5 nm unit to produce a hexagonal lattice when tessellated. A single unit of the tessellated grid is outlined in blue. This gives a skyrmion density of 0.61 skyrmions per square micrometer. Different skyrmion sizes are shown at the same density as (a), with diameters (b) 175 nm, (c) 515 nm, (d) 1008 nm, and (e) 1140 nm. (f) A 3000 × 5195 nm unit with 846 nm diameter skyrmions, giving a density of 0.13 skyrmions per square micrometer.

energy is found without using the precessional term in the Landau–Lifschitz–Gilbert equation. By running simulations with skyrmions of different sizes [as shown in Figs. 1(b)–1(e)], the global minimum can be found. This procedure is used because the solver easily finds the local minimum (which largely involves modifying spins in the domain wall) but it does not easily find the global minimum if there are small energy differences between skyrmions of similar sizes. Because of the effective hexagonal lattice created in the simulations, the position of the skyrmions does not change during the relaxation procedure. To study the effect of skyrmion density, simulations are run using different numbers of cells in the x- and y-directions. An example is shown in Fig. 1(f), where skyrmions are simulated at the same size as in Fig. 1(a), but with a density of 0.13 skyrmions/μm^2, as opposed to 0.61 skyrmions/μm^2 in Fig. 1(a).
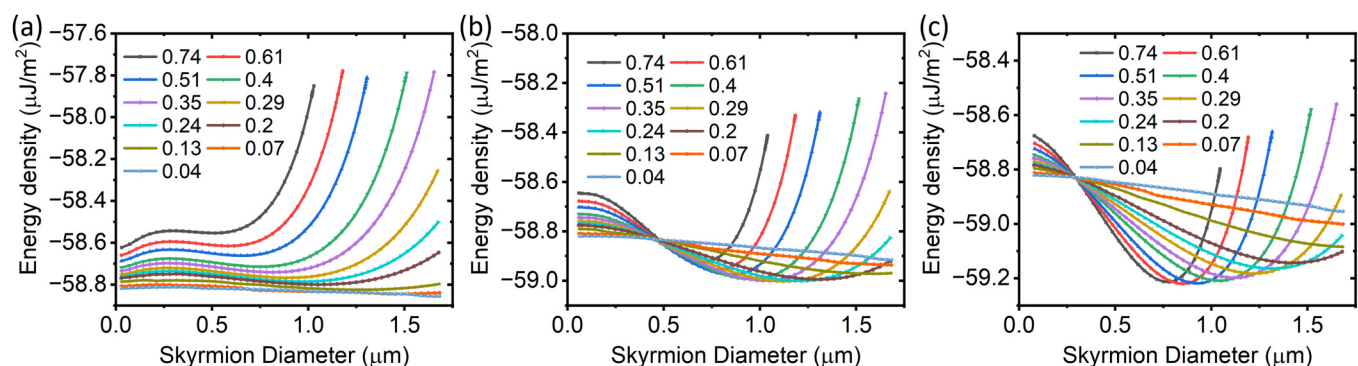

FIG. 2. Areal energy density extracted from the simulation as a function of the relaxed skyrmion diameter for different skyrmion densities (given in skyrmions/μm^2). In all three panels, the uniaxial anisotropy, K_u, is 9.82×10^5 J/m^3, with the DMI given by (a) 0.725 mJ/m^2, (b) 0.815 mJ/m^2, and (c) 0.875 mJ/m^2.

Periodic boundary conditions are used to create a similar effective area for all the simulations of around $172 \times 298 \ \mu m^2$, by adjusting the number of lateral repetitions. The diameter of the skyrmions is extracted from the simulations after the relaxation procedure. For skyrmions that are not round, such as those in Fig. 1(e), the diameter indicates the equivalent circular area of the skyrmion.

III. RESULTS

Figure 2 summarizes the simulation results. The areal energy density as a function of the skyrmion diameter is shown for different skyrmion densities. The panels in Fig. 2 show the results for different values of DMI, holding the other parameters constant. In general, the shape of individual curves is similar to those found for isolated skyrmions (see, e.g., Ref. 5). Figure 2(a) shows the results for a low DMI value of $0.725 \ mJ/m^2$ for which the skyrmion state is not energetically favorable. In this case, the energy density increases with increasing skyrmion density. The minimum energy density occurs for skyrmions simulated at the largest size and at the lowest density. The largest skyrmions considered here are around $1.6 \ \mu m$ in diameter, with the trend of the energy density indicating that the energy will be further minimized by even larger skyrmions. At these sizes, the system may be better described as a multidomain state, rather than a skyrmion state.

In Fig. 2(b), the energy density as a function of skyrmion size is shown for a system with a larger DMI of $0.815 \ mJ/m^2$. Now there is a more pronounced energy minimum for the skyrmion states, which is lower in energy density than the uniformly magnetized state ($-58.81 \ \mu J/m^2$ for all simulations in this figure). A minimum in the energy density is attained for skyrmion diameters between $0.7 \ \mu m$ and $1.3 \ \mu m$ with a range of skyrmion densities having similar energy minima. For this parameter set, there is a clear relationship between the size and density of the skyrmions with denser lattices comprising smaller skyrmions. In Fig. 2(c), the DMI is increased further leading to a more pronounced minimum in the areal energy density and a shift of the minimum energy to smaller skyrmion diameters for the same skyrmion densities as in Fig. 2(b). Notably, the observed decrease in the skyrmion size with increasing DMI is opposite to what has been simulated for a single, isolated skyrmion.[22]

The exchange constant, A_{ex}, also strongly affects the skyrmion size,[22] and skyrmions are generally expected to be more stable for lower A_{ex}. In Fig. 3, the exchange constant is changed by either reducing it by 10% [Fig. 3(a)] or increasing by 10% [Fig. 3(b)] relative to the simulations in Fig. 2(c). For the reduced exchange constant, the most notable change is in the energy density, with the minimum relating to the densest skyrmion state becoming deeper, even though the skyrmion size at the minimum does not change significantly. For the increased exchange used in Fig. 3(b), the minimum energy shifts to less dense but larger skyrmions, similar to the effect of reducing DMI seen in Fig. 2.

Simulations similar to those in Figs. 2 and 3 are carried out for a range of anisotropy and DMI values using the same value for the exchange constant as in Fig. 2. Figure 4 shows results where the skyrmion diameter [Fig. 4(a)] and density [Fig. 4(b)] at the minimum energy are extracted. For example, from the data in Fig. 2(c) a point with a skyrmion diameter of $0.85 \ \mu m$ and a
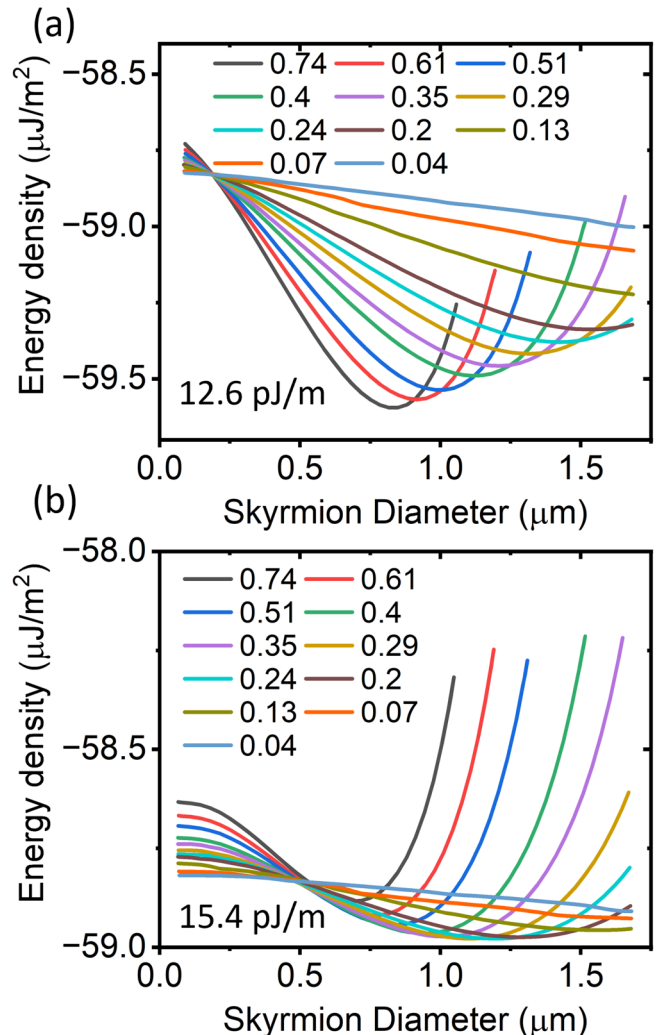

FIG. 3. Areal energy density extracted from the simulation as a function of the relaxed skyrmion diameter for different skyrmion densities (given in skyrmions/μm^2) with an exchange constant of (a) 12.6 pJ/m and (b) 15.4 pJ/m. In both panels, the uniaxial anisotropy, K_u, is $9.82 \times 10^5 \ J/m^3$ and the DMI is $0.875 \ mJ/m^2$ as in Fig. 2(c).

density of 0.61 skyrmions/μm^2 is found for $K_u = 9.82 \times 10^{-5} \ J/m^3$ and DMI of $0.875 \ mJ/m^2$. For some of the simulations, the skyrmion state with minimum energy is not well defined in the range of the simulations. In the bottom right corner of Fig. 4(a), the dark gray area corresponds to solutions where the lowest energy state is the smallest skyrmion size in the simulations which is found in the least dense lattice considered, as seen in Fig. 4(b).

For lower values of magnetic anisotropy and higher values of DMI, moving toward the top left corner of both graphs, it can be seen that the skyrmion diameter rapidly decreases in parallel with a rapid increase in the skyrmion density, demonstrating a strong correlation between these two parameters.

The change in skyrmion density as a function of anisotropy or DMI produces diodic-like non-linear functions.[10] The skyrmion density is fairly flat as a function of K_u or DMI in the bottom right corner of Fig. 4(b) but it increases linearly as the anisotropy is decreased or the DMI is increased. This is similar to the rectified linear activation (ReLU) function widely used in neuromorphic computing applications.[28] In Fig. 4(c), the filling factor of the skyrmions, given by the fractional area covered by skyrmions, is shown for these simulations. In the direction of low K_u and high DMI, the increased density of skyrmion leads to an increase in the filling factor—that is, it is not completely offset by the reduction in the skyrmion size.

In Fig. 4(d), the results of a different set of simulations are shown where skyrmions are nucleated in the center of a 2048×2048 cell. Periodic boundary conditions create a square lattice with a density of 0.04 skyrmions/μm^2 in this case, similar to the lowest

skyrmion density in the hexagonal lattices considered in Figs. 2 and 4. For the square lattice, the local energy minimum of the skyrmion state is found and the skyrmion diameter is extracted. The results indicate that in the region where skyrmions are stable their diameter is smaller than in the hexagonal array. This likely shows that the skyrmion size is sensitive to small differences in the dipolar fields caused by the difference in the coordination and nearest neighbor distance between square and hexagonal lattices. Despite these differences, the region of skyrmion stability in Fig. 4(d) occupies a similar parameter space to the region of the lowest skyrmion density as found in Fig. 4(b). The skyrmion densities in these two simulations are similar (around 0.04 skyrmions/μm^2) and the density is low enough that the simulations are a reasonable approximation to an isolated skyrmion in an extended film. This shows that an increased skyrmion density is required to stabilize skyrmions in the high DMI/low anisotropy part of the graph.
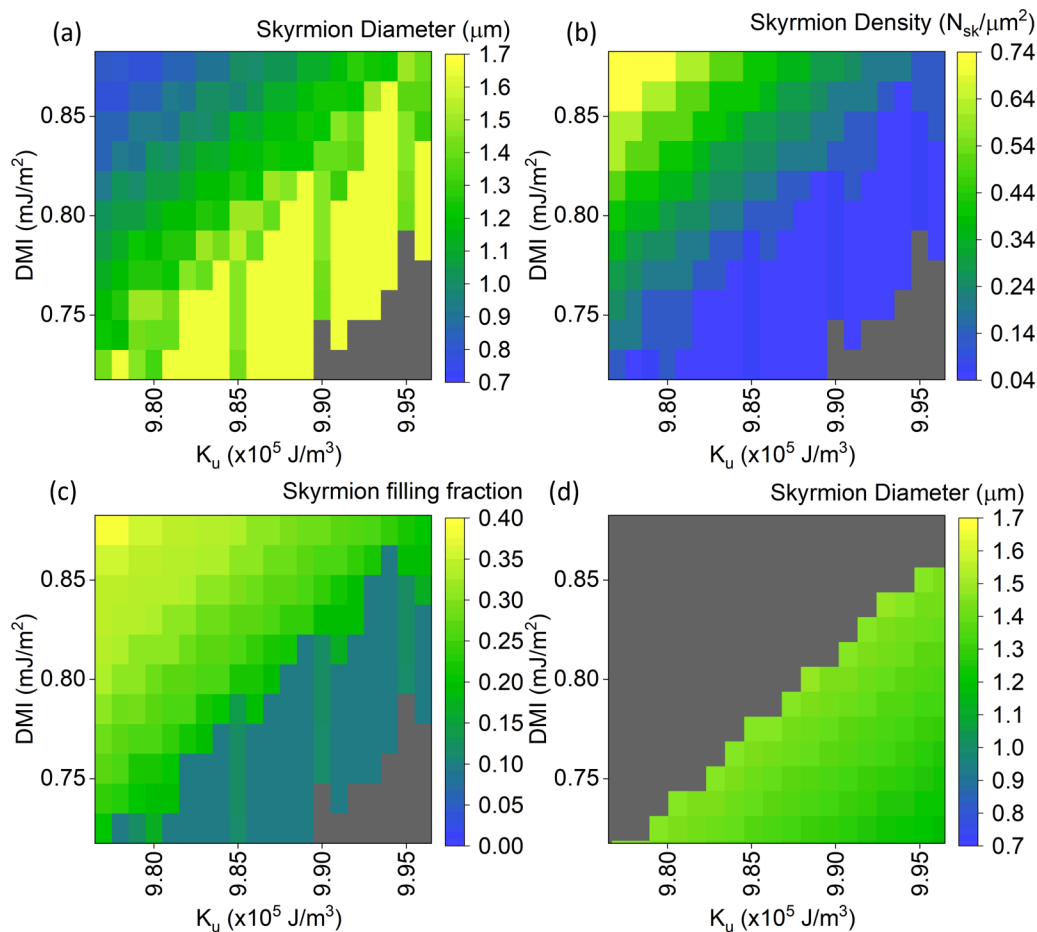

FIG. 4. (a) Skyrmion diameter found at the density with the minimum energy as a function of magnetic anisotropy and DMI. (b) Skyrmion density with the minimum energy as a function of magnetic anisotropy and DMI. (c) The spatial filling factor is given by the fraction of the total area covered by skyrmions as a function of magnetic anisotropy and DMI. (d) Simulation results for the skyrmion diameter on a square lattice at a density of 0.04 skyrmions/μm^2 (similar to the least dense hexagonal lattice). The skyrmion diameter is plotted as a function of magnetic anisotropy and DMI.

In the previous figures, the simulations did not incorporate any form of defects as typically found in thin film systems. Material systems studied for the voltage control of magnetism tend to be sputter-grown with polycrystalline layers. The effect of a granular film structure on skyrmion properties has been widely studied.[9,19,29,30] Typically in these studies, the grains are assumed to affect the magnetic anisotropy or DMI of the individual grains,
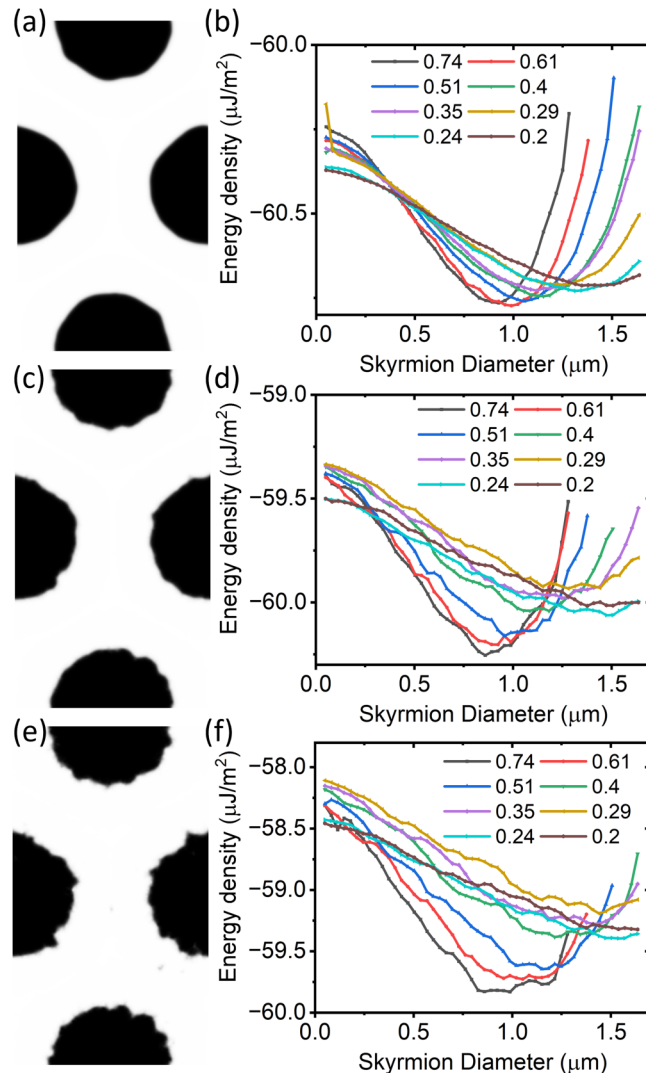

FIG. 5. (a) Simulation snapshot for a skyrmion lattice with 1% variation in anisotropy. The center of the anisotropy distribution is 9.84×10^5 J/m^3 and the DMI is 0.875 mJ/m^2. (b) Areal energy density extracted from the simulation in (a) as a function of the relaxed skyrmion diameter for different skyrmion densities (given in skyrmions/μm^2) for 1% variation in anisotropy. The data are the average of five simulations. (c) As (a) but with 5% variation. (d) As (b) but with 5% variation. (e) As (a) but with 10% variation. (f) As (b) but with 10% variation. Note the different energy density scales.

where typically the anisotropy or DMI is randomly drawn from a Gaussian distribution.[19,29] The grains are produced by a Voronoi process where the average grain size is specified. Here, an average of 10 nm grain is used. This approach is used in Fig. 5 in order to understand the effect of grains on the size and density of skyrmions. In Fig. 5(a), a snapshot of a simulation with grains, where the anisotropy of each grain is taken from a Gaussian distribution with a variation of 1%, is shown. As can be seen in the figure, the variation in anisotropy causes some noticeable deviations from circularity in the skyrmion shape. The plot of the areal energy density vs skyrmion diameter, shown in Fig. 5(b) for different skyrmion densities, shows well-defined minima with a global minimum for the second highest density. The energies shown are determined by the average of five simulations, which use a different initialization of the grains. The skyrmion diameter is calculated by finding the average area of the skyrmions and giving the equivalent diameter of a circle of the same area. If the variation in anisotropy is increased to 5%, as shown in Fig. 5(c), the increased edge roughness of the skyrmions is apparent. Comparing the skyrmion energy density in Fig. 5(d) to that in Fig. 5(b), several features are noticeable. First, the whole energy of the simulation is shifted upwards. Second, the minimum energy state is now associated with the highest density of skyrmions simulated, although it is not well-distinguished from the next highest density given the variation in the simulations. Third, the depth of the minimum associated with the skyrmion state is greater than in the preceding case. If the variation of the anisotropy is changed to 10%, the skyrmions, as shown in Fig. 5(e), become significantly rougher. This is again associated with a general increase in the energy of the skyrmions state as shown in Fig. 5(f). Also, the energy minimum density is now clearly associated with the densest skyrmion state. The size of the skyrmions at the minimum energy remains roughly the same with increasing variation in anisotropy.

IV. DISCUSSION

This study was motivated by the finding that the skyrmion density can be continuously controlled in experiments exploiting the voltage control of magnetism.[17] The results of the simulations are consistent with the changes in size and density seen experimentally assuming that the voltage causes changes in the anisotropy, DMI, or a combination of both on the scale of 1%–2%. It is clear that changing the magnetic anisotropy or DMI allows the size and density of skyrmions to be changed and that this process is not altered by the inclusion of an anisotropy variation. An interesting feature of this is the reversal of the trends seen for isolated skyrmions in terms of the skyrmion diameter. For isolated skyrmions, it has been found that increasing anisotropy or decreasing DMI leads to smaller skyrmions.[22] Here, as has been found previously,[23,24] we see that in dense lattices decreasing the anisotropy or increasing the DMI leads to smaller skyrmions. This has implications for using the skyrmion size as a key parameter in determining the DMI constant, for instance, if other material parameters are known, since it depends strongly on the skyrmion density.

The drivers of this behavior are loosely ascribed to the balance between dipolar fields and the domain wall energy. For the set of parameters considered here, the domain wall energy, given by

$4\sqrt{A_{ex}K_{eff}} - \pi D$, where K_{eff} is the effective anisotropy given by $K_{eff} = K_u - 0.5\mu_0 M_s^2$, is always positive and D is the DMI strength. Skyrmion lattices are also characterized[31] by the parameter $\kappa = \pi D / 4\sqrt{AK_{eff}}$, which is always less than 1 for the set of parameters used here. In the simulations shown here, the value of κ varies from ~ 0.5 to ~ 0.8 from high anisotropy/low DMI to low anisotropy/high DMI with the crossover to a dense lattice occurring for $\kappa \simeq 0.7$. Here, the crossover occurs well below $\kappa = 1$, which is sometimes stated to be the boundary between isolated skyrmions and lattice phases.[22,31,32] The derivation of κ assumes that the demagnetization energy can be approximated by setting $K_{eff} = K_u - 0.5\mu_0 M_s^2$. This assumption is valid for a uniformly magnetized thin film and has been successfully applied to the case of isolated skyrmions.[22] However, similarly to the calculation of stripe domain widths,[33] the demagnetization energy for a dense skyrmion array cannot be simply approximated and therefore $\kappa = 1$ does not necessarily represent a physical boundary between lattice and non-lattice phases. For decreasing anisotropy or increasing DMI, the domain wall energy reduces, and the equilibrium shifts to a denser skyrmion lattice with smaller skyrmions, which reduces the dipolar energy at the expense of increased domain wall length. In experiments, this effect can also be recognized without imaging by an increasingly slanted out-of-plane hysteresis loop that saturates at higher fields.

The addition of a granular structure with a variation in anisotropy strength leads to the minimum energy shifting to a denser skyrmion lattice. Considering again the domain wall energy, the rougher edge of the domain wall allows the wall to preferentially sit on lower anisotropy grains, minimizing the total energy. The effect of disorder is, therefore, to also shift the value of κ at which the crossover to a skyrmion lattice state occurs. Second, increasing the ratio of the perimeter to the area leads to a further reduction of the dipolar energy of the system as the dipole fields are largest closer to the domain boundaries in perpendicularly magnetized systems. That the roughness follows the grain size, here on average 10 nm, adds further complications to determining magnetic parameters from the skyrmion size, as this will depend on the typical scale of the roughness, which is difficult to image on these length scales.

Here, a strictly ordered lattice has been investigated. In experimental situations, disordered lattices and amorphous arrangements of skyrmions are often found,[19,34] where such arrangements can be driven by temperature[34] or material disorder.[19] The recent experiments on voltage control of skyrmions which prompted this investigation[17] show control of the skyrmion density, not in a well-defined lattice, but in a disorder driven amorphous skyrmion array. This indicates that a strong disorder is not enough to change the existence of the effects shown here, although it is likely that the size and density of skyrmions for any given set of magnetic parameters will be altered by the extent of the disorder. A further difference to experiments is the use here of 0 K simulations. Adding in the effects of temperature is likely to modify the skyrmion interactions.[35,36]

The results shown here support the possibility of using the skyrmion density as a parameter in neuromorphic devices. External control, through voltages for example, can be used to alter the anisotropy and DMI leading to non-linear changes in the skyrmion density, which span more than an order of magnitude. Only one small part of the very large parameter space where skyrmions are present was explored here and the size of the density changes seen here can likely be enlarged through the optimization of the relevant parameters.

AUTHOR DECLARATIONS
Conflict of Interest

The authors have no conflicts to disclose.

Author Contributions

Rhodri Mansell: Conceptualization (equal); Investigation (equal); Software (equal); Supervision (equal); Writing – original draft (equal); Writing – review & editing (equal). **Joonatan Huhtasalo:** Conceptualization (equal); Investigation (equal); Software (equal); Writing – review & editing (equal). **Maria Ameziane:** Conceptualization (equal); Supervision (equal); Writing – review & editing (equal). **Sebastiaan van Dijken:** Conceptualization (equal); Funding acquisition (equal); Supervision (equal); Writing – review & editing (equal).

DATA AVAILABILITY

The data that support the findings of this study are available from the corresponding author upon reasonable request.

REFERENCES

[1]A. Fert, V. Cros, and J. Sampaio, "Skyrmions on the track," Nat. Nanotechnol. **8**, 152–156 (2013).

[2]S. Woo, K. Litzius, B. Krüger, M.-Y. Im, L. Caretta, K. Richter, M. Mann, A. Krone, R. M. Reeve, M. Weigand, et al., "Observation of room-temperature magnetic skyrmions and their current-driven dynamics in ultrathin metallic ferromagnets," Nat. Mater. **15**, 501–506 (2016).

[3]W. Jiang, P. Upadhyaya, W. Zhang, G. Yu, M. B. Jungfleisch, F. Y. Fradin, J. E. Pearson, Y. Tserkovnyak, K. L. Wang, O. Heinonen, et al., "Blowing magnetic skyrmion bubbles," Science **349**, 283–286 (2015).

[4]W. Jiang, X. Zhang, G. Yu, W. Zhang, X. Wang, M. B. Jungfleisch, J. E. Pearson, X. Cheng, O. Heinonen, K. L. Wang, et al., "Direct observation of the skyrmion Hall effect," Nat. Phys. **13**, 162–169 (2017).

[5]M. Schott, A. Bernand-Mantel, L. Ranno, S. Pizzini, J. Vogel, H. Béa, C. Baraduc, S. Auffret, G. Gaudin, and D. Givord, "The skyrmion switch: Turning magnetic skyrmion bubbles on and off with an electric field," Nano Lett. **17**, 3006–3012 (2017).

[6]Y. Zhou, R. Mansell, and S. van Dijken, "Driven gyrotropic skyrmion motion through steps in magnetic anisotropy," Sci. Rep. **9**, 6525 (2019).

[7]Y. Zhou, R. Mansell, and S. van Dijken, "Voltage control of skyrmions: Creation, annihilation, and zero-magnetic field stabilization," Appl. Phys. Lett. **118**, 172409 (2021).

[8]X. Wang, W. L. Gan, J. C. Martinez, F. N. Tan, M. B. A. Jalil, and W. S. Lew, "Efficient skyrmion transport mediated by a voltage controlled magnetic anisotropy gradient," Nanoscale **10**, 733–740 (2018).

[9]C. Reichhardt, C. J. O. Reichhardt, and M. V. Milošević, "Statics and dynamics of skyrmions interacting with disorder and nanostructures," Rev. Mod. Phys. **94**, 035005 (2022).

[10]M. Cucchi, S. Abreu, G. Ciccone, D. Brunner, and H. Kleemann, "Hands-on reservoir computing: A tutorial for practical implementation," Neuro Comput. Eng. **2**, 032002 (2022).

[11]K. M. Song, J.-S. Jeong, B. Pan, X. Zhang, J. Xia, S. Cha, T.-E. Park, K. Kim, S. Finizio, J. Raabe, J. Chang, Y. Zhou, W. Zhao, W. Kang, H. Ju, and S. Woo, "Skyrmion-based artificial synapses for neuromorphic computing," Nat. Electron. **3**, 148–155 (2020).

[12]T. Yokouchi, S. Sugimoto, B. Rana, S. Seki, N. Ogawa, Y. Shiomi, S. Kasai, and Y. Otani, "Pattern recognition with neuromorphic computing using magnetic field-induced dynamics of skyrmions," Sci. Adv. **8**, eabq5652 (2022).

[13]Y. Sun, T. Lin, N. Lei, X. Chen, W. Kang, Z. Zhao, D. Wei, C. Chen, S. Pang, L. Hu, L. Yang, E. Dong, L. Zhao, L. Liu, Z. Yuan, A. Ullrich, C. H. Back, J. Zhang, D. Pan, J. Zhao, M. Feng, A. Fert, and W. Zhao, "Experimental demonstration of a skyrmion-enhanced strain-mediated physical reservoir computing system," Nat. Commun. **24**, 3434 (2023).

[14]Y. Wang, L. Wang, J. Xia, Z. Lai, G. Tian, X. Zhang, Z. Hou, X. Gao, W. Mi, C. Feng, *et al.*, "Electric-field-driven non-volatile multi-state switching of individual skyrmions in a multiferroic heterostructure," Nat. Commun. **11**, 3577 (2020).

[15]T. Srivastava, M. Schott, R. Juge, V. Krizakova, M. Belmeguenai, Y. Roussigné, A. Bernand-Mantel, L. Ranno, S. Pizzini, S.-M. Chérif, A. Stashkevich, S. Auffret, O. Boulle, G. Gaudin, M. Chshiev, C. Baraduc, and H. Béa, "Large-voltage tuning of Dzyaloshinskii–Moriya interactions: A route toward dynamic control of skyrmion chirality," Nano Lett. **18**, 4871–4877 (2018).

[16]C. Ma, X. Zhang, J. Xia, M. Ezawa, W. Jiang, T. Ono, S. Piramanayagam, A. Morisako, Y. Zhou, and X. Liu, "Electric field-induced creation and directional motion of domain walls and skyrmion bubbles," Nano Lett. **19**, 353–361 (2018).

[17]M. Ameziane, J. Huhtasalo, L. Flajšman, R. Mansell, and S. van Dijken, "Solid-state lithium ion supercapacitor for voltage control of skyrmions," Nano Lett. **23**, 3167–3173 (2023).

[18]D. M. Burn, S. Wang, W. Wang, G. van der Laan, S. Zhang, H. Du, and T. Hesjedal, "Field and temperature dependence of the skyrmion lattice phase in chiral magnet membranes," Phys. Rev. B **101**, 014446 (2020).

[19]R. Mansell, Y. Zhou, K. Kohvakka, S.-C. Ying, K. R. Elder, E. Granato, T. Ala-Nissila, and S. van Dijken, "Weakly pinned skyrmion liquid in a magnetic heterostructure," Phys. Rev. B **106**, 054413 (2022).

[20]L. Wang, C. Liu, N. Mehmood, G. Han, Y. Wang, X. Xu, C. Feng, Z. Hou, Y. Peng, X. Gao, and G. Yu, "Construction of a room-temperature Pt/Co/Ta multilayer film with ultrahigh-density skyrmions for memory application," ACS. Appl. Mater. Interfaces **11**, 12098–12104 (2019).

[21]S. Zhang, J. Zhang, Y. Wen, E. M. Chudnovsky, and X. Zhang, "Creation of a thermally assisted skyrmion lattice in Pt/Co/Ta multilayer films," Appl. Phys. Lett. **113**, 192403 (2018).

[22]X. Wang, H. Yuan, and X. Wang, "A theory on skyrmion size," Commun. Phys. **1**, 31 (2018).

[23]X.-C. Hu, H.-T. Wua, and X. R. Wang, "A theory of skyrmion crystal formation," Nanoscale **14**, 7516 (2022).

[24]H. Zhang, D. Raftrey, Y.-T. Chan, Y.-T. Shao, R. Chen, X. Chen, X. Huang, J. T. Reichanadter, K. Dong, S. Susarla, L. Caretta, Z. Chen, J. Yao, P. Fischer, J. B. Neaton, W. Wu, D. A. Muller, R. J. Birgeneau, and R. Ramesh, "Room-temperature skyrmion lattice in a layered magnet $(Fe_{0.5}Co_{0.5})_5GeTe_2$," Sci. Adv. **8**, eabm7103 (2022).

[25]Y. Zhou, R. Mansell, T. Ala-Nissila, and S. van Dijken, "Thermal motion of skyrmion arrays in granular films," Phys. Rev. B **104**, 144417 (2021).

[26]A. Vansteenkiste, J. Leliaert, M. Dvornik, M. Helsen, F. Garcia-Sanchez, and B. Van Waeyenberge, "The design and verification of MuMax3," AIP. Adv. **4**, 107133 (2014).

[27]J. Mulkers, B. Van Waeyenberge, and M. V. Milošević, "Effects of spatially-engineered Dzyaloshinskii-Moriya interaction in ferromagnetic films," Phys. Rev. B **95**, 144401 (2017).

[28]V. Vadde, B. Muralidharan, and A. Sharma, "Power efficient ReLU design for neuromorphic computing using spin Hall effect," J. Phys. D: Appl. Phys. **56**, 415001 (2023).

[29]J.-V. Kim and M.-W. Yoo, "Current-driven skyrmion dynamics in disordered films," Appl. Phys. Lett. **27**, 132404 (2017).

[30]R. Juge, S.-G. Je, D. de Souza Chaves, S. Pizzini, L. D. Buda-Prejbeanu, L. Aballe, M. Foerster, A. Locatelli, T. O. Menteş, A. Sala, F. Maccherozzi, S. S. Dhesi, S. Auffret, E. Gautier, G. Gaudin, J. Vogel, and O. Boulle, "Magnetic skyrmions in confined geometries: Effect of the magnetic field and the disorder," J. Magn. Magn. Mater. **455**, 3–8 (2018).

[31]M. Raju, A. P. Petrović, A. Yagil, K. S. Denisov N. K. Duong, B. Göbel, E. Şaşıoğlu, O. M. Auslaender, I. Mertig, I. V. Rozhansky, and C. Panagopoulos, "Colossal topological Hall effect at the transition between isolated and lattice-phase interfacial skyrmions," Nat. Commun. **12**, 2758 (2021).

[32]F. Ajejas, Y. Sassi, W. Legrand, T. Srivastava, S. Collin, A. Vecchiola, K. Bouzehouane, N. Reyren, and V. Cros, "Densely packed skyrmions stabilized at zero magnetic field by indirect exchange coupling in multilayers," APL. Mater. **11**, 061108 (2023).

[33]I. Lemesh, F. Büttner, and G. S. D. Beach, "Accurate model of the stripe domain phase of perpendicularly magnetized multilayers," Phys. Rev. B **95**, 174423 (2017).

[34]P. Huang, T. Schönenberger, M. Cantoni, L. Heinen, A. Magrez, A. Rosch, F. Carbone, and H. M. Rønnow, "Melting of a skyrmion lattice to a skyrmion liquid via a hexatic phase," Nat. Nanotechnol. **15**, 761–767 (2020).

[35]C. Reichhardt and C. J. O. Reichhardt, "Peak effect, melting, and transport in skyrmion crystals," Phys. Rev. B **108**, 014428 (2023).

[36]Y. Wang, J. Wang, T. Kitamura, H. Hirakata, and T. Shimada, "Exponential temperature effects on skyrmion-skyrmion interaction," Phys. Rev. Appl. **18**, 044024 (2022).